On Scattering Coefficients and Fitting Density for Room Acoustic Simulation of Industry Halls

Thomas Ziegler
Ziegler Schallschutz GmbH, 5020 Salzburg, E-Mail: ziegler@ziegler-schallschutz.at

1. Introduction

Performing simulations with Geometrical Acoustics (GA) means creating a simplified model of a room's acoustically relevant objects and assigning absorption and scattering coefficients to surfaces. Absorption and scattering coefficients should be based on physical reasoning taking into account surface roughness, size, shape and exposure. For real working rooms having complex internal fittings in terms of furniture, machines, beams and ducts this reasoning is especially difficult due to multiple uncertainties when transforming room-properties into a model suitable for GA:

- Level of detail to model a room and its internal fittings [1] [2]. Basically, the required level of geometric detail is inversely proportional to room size and distance of structures to sources and receivers. Fine details should be omitted to avoid creation of a model suited only for high frequencies. The lower level of detail should be compensated by increased surface scattering coefficients.
- Data sheets showing absorption coefficients for a range of construction materials and sound absorbers are usually available. Scattering coefficients of real room-boundaries having various exposures and structures, however, are hard to guess but significantly influence results in case of high and uneven absorption and non mixing room geometries.
- Absorption and scattering coefficients of complex fittings in workrooms are generally unknown and hard to estimate by visual inspection. In densely equipped rooms these structures have a major effect on the sound field.
- Sound power and directivity characteristics of sound sources (e.g noisy parts of production machines in industry halls) are often unknown.

Round Robin Studies [3-6] comparing simulation and measurement results show significant deviations due to inconsistent interpretation of uncertainties by software users even for rather simple rooms. A real industry hall, however, provides a degree of uncertainty such that rule of thumb estimations of input data seem unrealistic given the accuracy expected by customers having to match labour laws concerning noise exposition of employees and mean absorption degrees of rooms.

In case of acoustical renovation projects, however, we may hope to alleviate the problem of inaccurate input data by calibrating the simulation model to approximate acoustical measurements of the untreated room prior to investigating the effect of acoustical treatments. [7] shows a detailed procedure for model calibration and its application to a cathedral. The model calibration approach can be outlined as follows:

- Input parameters are initialized based on measurement of object dimensions, physical reasoning, and material data-sheets with maximum possible accuracy.
- The untreated room is simulated and input parameters are calibrated until the difference between simulation- and measurement result is smaller than some target value
- Finally, the effect of the acoustical treatment is predicted.

Note that model calibration suffers from an ambiguity problem, meaning that different sets of input parameters (e.g. combinations of absorption/scattering coefficients of multiple materials in a room) can result in the same value for the calibrated measure (e.g. T_{30}) possibly causing wrong prediction results. For instance, considering a room with an absorbent ceiling to be mounted, the same T_{30} can be achieved if calibrating the untreated room assuming a ceiling with rather high absorption and walls with rather low absorption or vice versa. In the first case the effect of the absorbent ceiling on T_{30} will be significantly smaller than in the second case. Thus keeping in mind physical reasoning during the calibration phase is of course essential.

[8] proposes a tool for controlled parameter variation in GA. [9] evaluates simulation accuracy for industrial noise control in several workplaces using model calibration. [10] investigates Sound Pressure Level (SPL) predictions in an industry hall using model calibration but does not compare simulation and measurement results after the acoustical treatment. [11] is a predecessor version of the present paper focusing on a least-effort empty room scenario as compared to a scenario with fittings. Detailed simulation parameter settings are different, however, and variation of fitting density is missing as compared to this paper.

2. Room Description and Measurement Setup

The considered room is a production hall with sawing and mortising machines for aluminum processing owned by Airambulance Technology GmbH in Ranshofen, Austria. The room has proportions of $30 \cdot 20 \cdot 4 m^3$; i.e. a flat working room. Measurements and the acoustical treatment were carried out in February 2018. Measurement parameters:

- Speaker height 1.6m. Mic height 1.3m
- Noise excitation for T_{30} measurements is performed with a pistol shot

− Loudspeaker: Norsonic 276. Amp: Norsonic NOR280, White Noise, Amp level -10dB; internal EQ activated

− Measurement device: B&K 2260, calibrated

− The background noise equals 45dB which is negligible compared to SPLs created for T_{30} and SPL measurements.

T_{30} measurement points are evenly distributed over the room. Receiver and source positions in measurement and simulation are identical.

In order to avoid the directional characteristics of the dodecahedron source at 2kHz and 4kHz octave bands, the speaker has been turned several times to measure average SPL in the near field of the source.

In order to evaluate spatial decay curves (SDC), SPLs are measured along two straight lines throughout the hall. SDC1 along the main corridor; SDC2 almost orthogonal to SDC1, see figure 1a. According to the recommendations in [12], measurement points are located in 1m intervals between 1m and 10m from the source and in 2m intervals up to 20m from the source. Measurement points and receiver locations in simulation are identical.

The acoustical treatment consists of melamine foam absorber panels glued on the ceiling and walls. The panels were mounted with a shadow gap of 5cm to each other. A total of 408m^2 have been mounted, 301m^2 with a format of 100·50·5cm^3 on the ceiling, 49m^2 with a format of 100·50·5cm^3 on walls and 58m^2 sized 100·50·7cm^3 on walls.

3. Research Question and Simulation Scenarios

For typical working rooms as considered in this paper high uncertainties will result in GA users showing high variation in setting scattering coefficients and fitting density. Thus we are interested in the sensitivity of GA results in case of extensively varying scattering coefficients and level of geometric detail.

Three scenarios are considered concerning geometrical detail:

− empty room without any internal fittings. Total surface[1] 1719m2.

− medium density (MD) with internal fittings considered having at least one edge > 2m. Surface of fittings 322m2. Total surface 1944m2.

− high density (HD), as shown in figure 1, with internal fittings considered having at least one edge > 1m. Surface of fittings 548m2. Total overall surface 2170m2.

For each level of geometric detail (empty, MD, HD) we examine a low (LS), a medium (MS), and a high scattering (HS) scenario. Subsequent paragraphs describe the approach to variation of scattering coefficients:

Simulations are performed with CATT-Acoustic, v9.1.a [13]. CATT-Acoustic's auto-edge scattering is a feature to automatically set scattering coefficients of freely exposed object surfaces in order to mimic edge diffraction by increased surface scattering. Scattering coefficients are set dependent on wavelength and surface size as well as shape.

[1] Note fittings cover space on the floor thus total surfaces in scenarios with different density cannot be compared directly.

Basically, auto-edge scattering results in higher scattering values for smaller and irregular surfaces and longer wavelengths. Typically, auto edge scattering computes coefficients > 90% for small surfaces and 125Hz octave band and < 10% percent for 4kHz.

For the present paper two issues have been considered concerning setting scattering coefficients. (1) to be able to compare results of the empty, medium and high density scenarios with respect to their stability concerning variation of scattering, the mean overall scattering coefficients (S_O) need to be identical for the low/medium/high scattering scenarios for the three levels of density for each octave band. Note that S_O is computed as the weighted average of per octave band scattering coefficients of all surfaces, where weights are the surface sizes. (2) the auto-edge scattering feature of CATT-Acoustic supports setting coefficients realistically thus we intend to enable it for fittings, but auto-edge computes an individual scattering coefficient for each surface and octave band, requiring an additional tool to be able to integrate both desirable aspects in our simulations.

Based on the surfaces used by CATT-Acoustic the tool allows definition of per octave band overall scattering coefficients (S_O) for the entire scenario (i.e. all surfaces) and surface scattering coefficients of fittings (S_{FS}) by the user. Based on surface scattering coefficients and CATT-Acoustic's auto-edge scattering formula the tool computes effective scattering coefficients of fitting surfaces (S_{FE}) and, subsequently, scattering coefficients for the residual hard surfaces like walls, floor and ceiling (S_r) such that the user defined overall scattering coefficients (S_O) for the entire scenario are achieved. Thus this approach combines the use of auto edge scattering and comparable overall scattering coefficients.

Scattering and absorption coefficients are shown in Table 1 and 2, respectively. Absorption coefficients of residual surfaces (walls, floor, ceiling) are the result of model calibration, matching measured and simulated T_{30} before installing the acoustical treatment. S_{FS} is set with an increase of 5% per octave band and a mean of 20% for LS, 47% for MS and 75% for HS scenarios. Based on the auto-edge scattering computation this results into mean effective scattering coefficients S_{FE} between 36 and 90%. Note that auto-edge scattering causes higher S_{FE} for low octave bands than for high octave bands. Mean S_O ranges from 26% for LS to 81% for HS scenarios and exhibits a moderate increase per octave band. Based on chosen input parameters (S_O, S_{FS}) and auto-edge scattering resulting S_r cover a wide range, between 9% for HDLS and 87% for HDHS.

We emphasize that the approach for setting scattering coefficients used in this paper is not what an acoustic consultant would usually do in a practical project; i.e. set scattering based on physical reasoning. On the contrary, our aim is (1) to evaluate the entire parameter space for scattering coefficients to understand better the sensitivity of GA results in case of possibly „wrong“ settings and (2) have well defined overall scattering (S_O) in order to be able to compare scenarios with different fitting densities (empty, MD, HD).

Further simulation parameter settings: Algorithm 1, Split order 0, diffraction disabled. $2 \cdot 10^6$ rays, ray tracing 2 seconds for the untreated room. $7 \cdot 10^6$ rays, 2 seconds ray tracing for the treated room. Note that due to its uneven and high absorption the treated scenario requires more rays to achieve echograms without artificial spikes in the late part of the sound decay. Various tests with other algorithms including advanced scattering methods and diffraction showed inferior echograms as compared to the settings above. Air absorption is enabled. E (Energy) values are used for evaluations. See [13] for detailed explanations of the simulation parameters mentioned above.

4. Measures

In Industrial noise control usually SPL reduction, reverberation time (T_{30}), and DL_2 -the SPL decay when doubling the distance to the source - are of interest. Let $L_{m,i,b}$ define the measured, and $L_{s,i,b}$ the simulated SPL at measurement point i before the acoustical treatment. Equivalently, $L_{m,i,a}$ and $L_{s,i,a}$ are defined after the acoustical treatment. Then SPL Calibration Error at point i (CE_i) is defined as

$$CE_i = |L_{m,i,b} - L_{s,i,b}| \quad (1)$$

Prediction Error at point i (PE_i) is defined as

$$PE_i = |L_{m,i,a} - L_{s,i,a}| \quad (2)$$

CE and PE, respectively, denote the mean over a set of measurement points. Let r define the distance between source and a measurement point. According to the recommendations in [11], DL_2 is computed in the near region $1 \leq r \leq 5$m and the middle region $5 \leq r \leq 16$m. On the contrary to SPL, where CE and PE are computed per measurement point, CE and PE of DL_2 are computed as the DL_2 difference between measurement and simulation over all measurement points in the near and middle region, respectively.

Similar to DL_2, T_{30} CE and PE are computed as the mean over all measurement points. Measurement points and receiver points in simulation have identical locations. During the model calibration phase absorption coefficients of the residual surfaces (see section 3) are tuned such that the T_{30} CE is minimal.

Whereas SPL and DL2 PEs are computed in dB, T30 errors are computed in percent of the mean measured value in order to enable comparison among PEs and CEs before and after the acoustical treatment.

Simulated SPLs are normalized during post processing such that measured and simulated SPLs at r=1m are identical. SPL normalization allows comparison of sound decays in different scenarios solely based on room properties for r > 1m, avoiding errors in modeling the dodecahedron source.

The Schroeder frequency of the untreated hall equals 53Hz. In order to take GAs limitations in the low frequency range into account we consider the frequency range between 250Hz and 4kHz. Note that LA_{eq} is computed over 250-4kHz octave bands in order to enable comparison between measurement and simulation results.

5. Reverberation Time

As shown in Figure 2a-c, as a result of model calibration T_{30} CEs are smaller than 3% in all scenarios. Figure 3 shows that T_{30} PEs are very high in case of the Empty-LS scenario (30% < PE < 50%). For Empty-MS, MDLS and HDHS scenarios T_{30} PEs are greater than 10%. There exists a medium range of setting scattering coefficients and fitting density (empty HS, MDMS, MDHS, HDLS, HDMS) with T_{30} PEs smaller than 10%.

Generally, scenarios with fittings (MD, HD) are significantly less sensitive to variation of scattering than the empty room scenario and show small T_{30} PEs in case scattering is neither set low nor extremely high.

As a rough indication for T30 values we mention that measured octave-band T30 ranges between 1.4 and 1.7 seconds before the acoustical treatment and 0,6 and 1 seconds after treatment.

6. Sound Pressure Levels

Figure 4 shows mean SDC1 CEs in dB. Figure 5 and 6 show SDC1 and SDC2 PEs for all measurement points as well as error bars with 10% and 90% quantiles. Evaluating figure 5 and 6 we find that SPL is generally less sensitive to variation of scattering and fitting density than T_{30}. We reason that the insensitivity of SPL as opposed to T_{30} is due to T_{30} having higher dependency on the late parts of impulse responses and Energy Time Curves than SPL. Furthermore, we find that

- SPL CE and, even more, SPL PE quantiles show high variation among measurement points. This is due to the simulated model not being capable of reproducing measured local SPL variation. See for instance the SDC1 500Hz band, HDMS scenario in Figure 5 with a 90% PE quantile of 4dB. Figure 7a shows the corresponding decay curve, indicating the reason for the high PE quantile. Between r=11m and r=14m from the source the measured SPL curve shows a spike, not followed by the simulated curve.[2] In case of a smooth SPL decay, simulated SDCs approximate measured SDCs very well. See for example Figure 7a, 1<r<11m or Figure 7b.

- Due to high per measurement point variances, mean PE and CE do not always correlate. See for instance SDC1, Figure 4 and 5, MDMS scenario, 1000Hz band. Mean SDC1 CE shows a maximum while mean PE is close to zero. This can be considered as an example for the ambiguity problem of model calibration. Different settings for scattering and levels of detail in modeling fittings may result in similar calibration errors but significantly different prediction errors.

- Mean octave-band SPL CEs are smaller than 1.5 dB, with 90% quantiles generally smaller than 2dB. Mean

[2] Note that the measured decay curve before carrying out the acoustical treatment (small points) shows the same spike - though less pronounced - as compared to the curve after the treatment. Measured decay curves in other octave bands in SDC1 and SDC2 show similar, though less pronounced behavior due to local SPL variation between neighboring measurement points.

octave-band SPL PEs are usually smaller than 2dB, with 90% quantiles smaller than 5dB for SDC1 and 3dB for SDC2. Maximum SPL PEs of 7dB at single measurement points and octaves were observed.

- Comparing per measurement point LAeq PE to octave band PEs, we observe that, obviously, sums over octaves tend to minimize PE (mean and quantile). Similarly, mean SDC1 and SDC2 PEs are smaller than per measurement point PEs as indicated by quantiles.
- We briefly mention that measured octave-band SPLs range from 70 to 105 dB dependent on the distance to the source, octave band and the overall absorption in the room.

7. Further Measures

Table 3 shows DL_2 CEs and PEs, where PEs > 1 are marked with grey background, PEs > 2 are marked with black background. Analyzing Table3 we find that DL_2 PEs are smaller than 1 dB in the near region and usually smaller than 2dB in the middle region. Similar to SPL results, no indication for strong dependency of DL_2 PEs on variation of scattering or fitting density can be observed. Local spikes or dips in measured SDs, however, cause higher DL_2 PEs in the middle region. See for instance, SDC1 PE, middle range, HDMS, 500Hz in Table 3 and figure 7.

Note that Dl_2 PEs in the range of 2db are significant given the fact that DL_2 ranges between 2 and 5 dB in usual rooms. Figure 8a shows middle range SDC1 DL_2 PE in [%] of the measured value as compared to DL_2 PE in [dB] in figure 8b. PEs in the range of 2.5 dB in figure 8b correspond to PEs of 80% in figure 8a.

Similar to SPL high Dl_2 PEs are caused by local deviations between measurement and simulation. At the 16m limit of the middle range the difference between measured and simulated SPL shows a maximum in figure 7a, causing a high DL_2 PE. Thus, according to the results of the considered room, Dl_2 is a rather difficult measure for predictions with GA. If the middle range was extended to 20m, the DL_2 PE of SDC1, middle range, HDMS, 500Hz would have been significantly smaller.

In February 2019 additional measurements were performed using Dirac [14], a class 1 USB microphone and the Norsonic dodecahedron speaker and Amplifier mentioned in section 2. This measurement setup enables investigation of additional measures and extended features for roomacoustical analysis. Concerning fittings and the installed sound absorbers, no changes were visible in the hall as compared to the measurements after the acoustical treatment one year earlier. Additionally, identical measurement points have been used as in 2018. SPL measurements performed at SDC1 and SDC2 measurement points confirm the measurement results in 2018.

The difference between T_{30} measurement result in 2019 as compared to 2018 is smaller or equal than 5% for all octave bands, see table 4. The differences may be due the use of sine sweeps in 2019 as compared to pistol shots in 2018. 5% deviation corresponds to differences in reverberation time measurements according to ISO 3382-2, standard class.

Figure 9 shows EDT PEs. Comparing results in Figure 9 and figure 3 supports section 6's reasoning concerning measures related to the late parts of the energy time curve of impulse responses showing higher sensitivity with respect to variation of fitting density and scattering coefficients as compared to measures related to the early part of energy time curves. The empty-LS scenario, for instance, shows T_{30} PEs in the range of 45% in figure 3 as compared to EDT PEs around 25% in figure 9. Similarly, T30 PE shows stronger dependency on variation of scattering-level and fitting density than EDT PE in the other scenarios.

Figure 10 shows T_{15} PEs. Results are in-line with the reasoning mentioned above. Considering the empty-LS scenario for instance, T_{15} PEs are in-between T_{30} and EDT.

Finally, figure 11 shows STI PEs. Measured STI ranges between 0.6 and 0.8 dependent on the distance between source and meaurement point. Mean STI PEs are smaller than 0.04, 90% quantiles smaller than 0.07 thus generally very small and insensitive to variation of fitting density and scattering. Consequently, for the considered room, STI is a very reliable measure to be predicted by GA.

8. Conclusions

Investigating the sensitivity of T_{30} simulation results with respect to variation of fitting density and scattering-level we find that there exists a medium range (empty HS, MDMS, MDHS, HDLS, HDMS) of scenarios with small T_{30} prediction errors. T_{30} prediction errors are very high in case of the empty room and low scattering scenario. Generally, scenarios with fittings are significantly less sensitive to variation of scattering than the empty room scenario and show small T_{30} PEs in case scattering is neither set low nor extremely high.

Considering SPL we find that prediction errors are generally independent of fitting density and scattering-level for the considered room. Although measured curves are generally approximated very well, GA is not always able to reproduce measured local SPL spikes or dips. Consequently, we find that per octave band SPL prediction errors may be significant at specific measurement points. Considering LA_{eq}, however, per measurement point errors tend to be sufficiently small for SPL prediction. The latter statement also holds for mean octave-band SPL computed over several measurement points.

In accordance with mean SPL results, Dl_2 prediction errors are insensitive with respect to variation of fitting density and scattering. Errors in the middle region are significantly higher than errors in the near region. In relation to measured values, Dl_2 prediction errors can be very high, see figure 8.

Investigating SPL, Early decay Time (EDT) and T_{15} PEs as compared to T_{30} PEs supports the hypothesis that measures related to the late parts of the energy decay following an impulse response show higher sensitivity with respect to variation of fitting density and scattering coefficients as compared to measures related to the early part of energy decay.

Finally, STI PEs are generally very small and insensitive to variation of fitting density and scattering. Thus STI provides reliable predictions for the considered scenarios.

We emphasize that results in this paper provide qualitative indications only for closely related scenarios and under the assumption of model calibration:

- flat room with dense fittings, similar size and proportions
- considered measures
- absorbent treatments on most walls and ceiling
- line of sight between sources and receivers.

The limitation to a single room encourages future comparative studies analyzing simulation errors in other working rooms by systematically investigating the multidimensional space of input parameters to geometrical acoustics. Combination of this knowledge might in the future result in expert systems and standards helping engineers to avoid pitfalls in acoustic simulation.

9. References

[1] M.Vorländer: Performance of Computer Simulation for Architectural Acoustics. Proceedings of 20th international Congress on Acoustics, ICA 2010, Sydney Australia.

[2] B.I. Dalenbäck: Engineering Principles and Techniques in Room Acoustics Prediction. BNAM 2010

[3] M. Vorländer: International Round-robin on Room Acoustical Computer Simulation. Proceedings of 15th ICA, Trondheim, Norway, 1995.

[4] I. Bork: A comparison of room simulation software - the 2nd round robin on room acoustical computer simulation" Acta Acustica, vol. 86, 2000.

[5] I. Bork: Report on the 3rd round robin on room acoustical computer simulation - Part I: Measurements Acta Acustica united with Acustica, vol. 91, 2005.

[6] I. Bork: Report on the 3rd round robin on room acoustical computer simulation - Part II: Calculations, Acta Acustica united with Acustica, vol. 91, 2005.

[7] B.N.J. Postma, B.F.G. Katz: Creation and calibration method of acoustical models for historic virtual reality auralizations, Springer Verlag London, 2015

[8] B.I. Dalenbäck, U.P. Svensson: A prediction software interface for room acoustic optimization, 19th International Congress on Acoustics, Madrid, 2007

[9] J. Keränen et. al.: Validity of ray tracing method for the application of noise control in workplaces. Acta Acustica united with Acustica, Vol. 89, 2003, 863-874

[10] Hodgson M.R. Case history: factory noise prediction using ray tracing: experimental validation and the effectiveness of noise control measures. Noise Control Engineering Journal, 33, 3, pp. 97-104, 1989-11

[11] T. Ziegler: Comparing measurement and simulation results using model calibration for room-acoustical evaluation of industry halls, EAA Euronoise 2018, June 2018, Crete, Greece

[12]ISO 14257 (1st ed. 2001): "Acoustics – Measurement and parametric description of spatial sound distribution curves in workrooms for evaluation of their acoustical performance"

[13] CATT-Acoustic, www.catt.se

[14] Dirac, Bruel & Kjaer, https://www.bksv.com/media/doc/bp1974.pdf

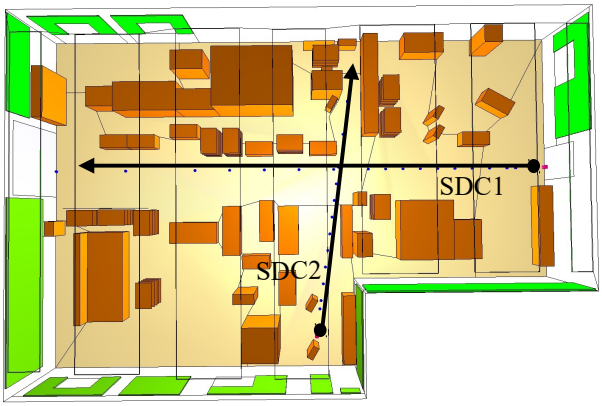

Figure 1a: High density (HD) model of the considered hall including fittings, sources, measurement points, sound absorbers on walls. Figure 1b. Medium Density (MD) scenario.

	S_0	S_0	S_O	S_{FS}	S_{FS}	S_{FS}	Gates	S_{FE}	S_{FE}	S_{FE}	S_{FE}	S_{FE}	S_{FE}	S_R	S_R	S_R	S_R	S_R	S_R	S_R	S_R	S_R
Scattering	LS	MS	HS	LS	MS	HS	all	LS	MS	HS	LS	MS	HS	LS	MS	HS	LS	MS	HS	LS	MS	HS
Density	all	all	all	all	all	all	all	MD	MD	MD	HD	HD	HD	empty	empty	empty	MD	MD	MD	HD	HD	HD
250	20	47	75	10	37	65	35	51	76	95	57	82	96	20	47	75	14	41	71	9	37	69
500	23	50	78	15	42	70	40	36	63	89	39	66	92	23	50	78	20	48	76	18	46	75
1000	26	53	81	20	47	75	45	30	57	85	32	59	87	26	53	81	25	52	81	24	51	80
2000	29	56	84	25	52	80	50	30	57	85	31	58	86	29	56	84	29	56	84	28	55	84
4000	32	59	87	30	57	85	55	33	60	88	33	60	88	32	59	87	32	59	87	31	59	87
Mean	26	53	81	20	47	75	45	36	63	88	39	65	90	26	53	81	24	51	80	22	50	79

Table 1: Scattering coefficients [%], grey as a result of tool

Surface	Gates	Absorber 5cm	Absorber 7cm	Fittings	Residual								
Scattering	all	all	all	all	LS	MS	HS	LS	MS	HS	LS	MS	HS
Density	all	all	all	all	empty	empty	empty	MD	MD	MD	HD	HD	HD
250	10	50	74	17	22	16	15	16	12	11,8	10,3	10,3	10,1
500	10	83	86	15	17	14	13	12,8	10,5	10,6	9,2	9,2	9,1
1000	10	86	86	13	14	12	12	10,6	9,5	9,5	8,2	8,2	8,1
2000	9	86	86	10	12	11	11	9,5	9,3	9,3	7,7	7,7	7,7
4000	8	86	86	10	11	10	10,5	9,1	8,3	8,3	7,4	7,4	7,4
Mean	9,4	78,2	83,6	13	15,2	12,6	12,3	11,6	9,9	9,9	8,6	8,6	8,5

Table 2: Absorption coefficients [%], grey as a result of model calibration

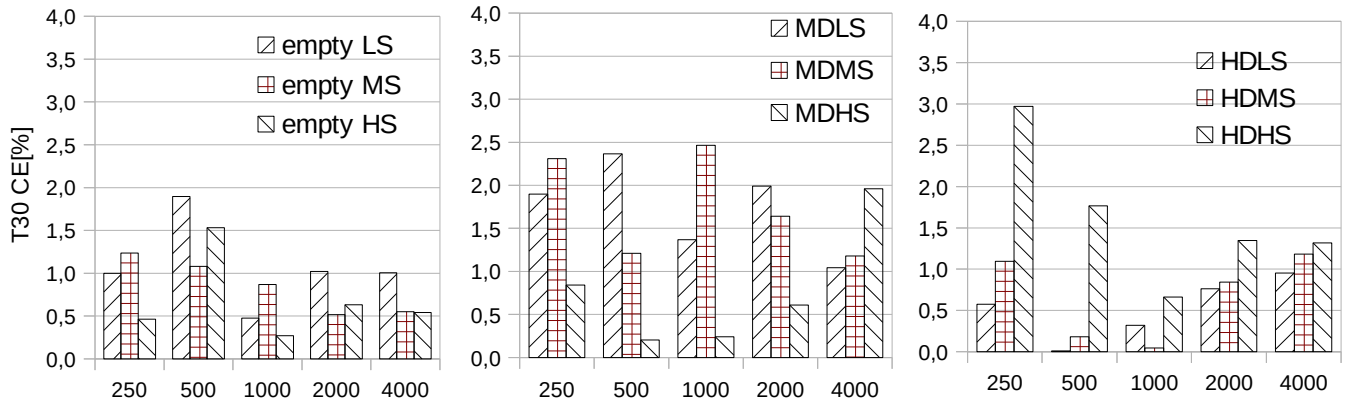

Figure 2 a,b,c: T_{30} Calibration Error [%]. Empty room, MD, HD scenario

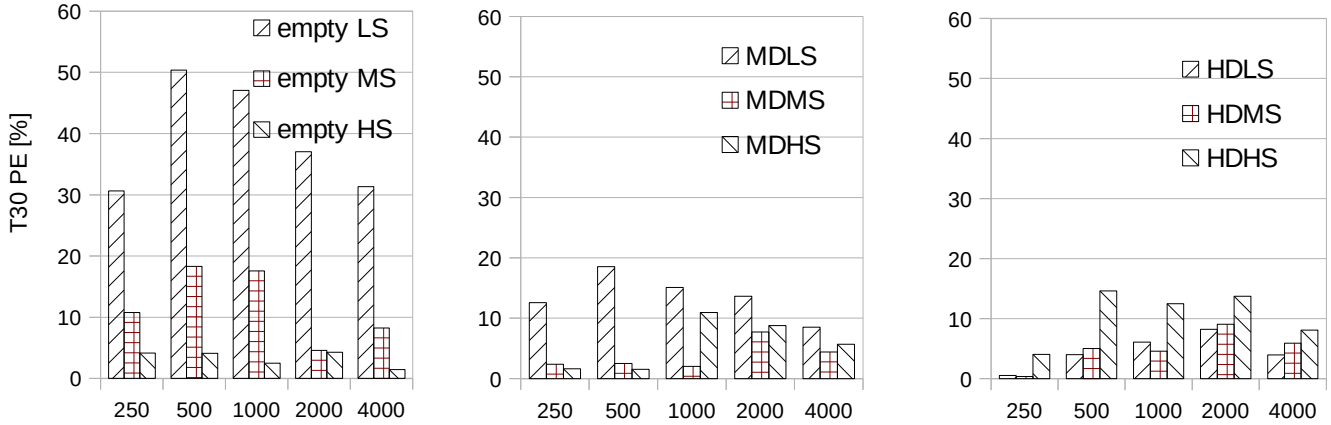

Figure 3a,b,c: T_{30} Prediction Error [%]. Empty room, MD, HD scenario

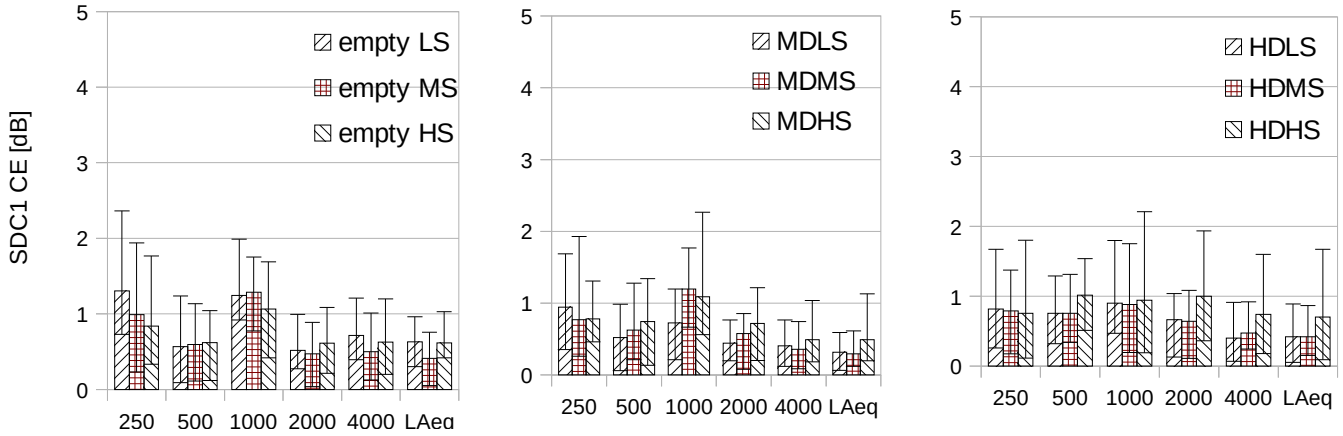

Figure 4 a-c: SDC1 Calibration Error [%]. Empty room, MD, HD scenario

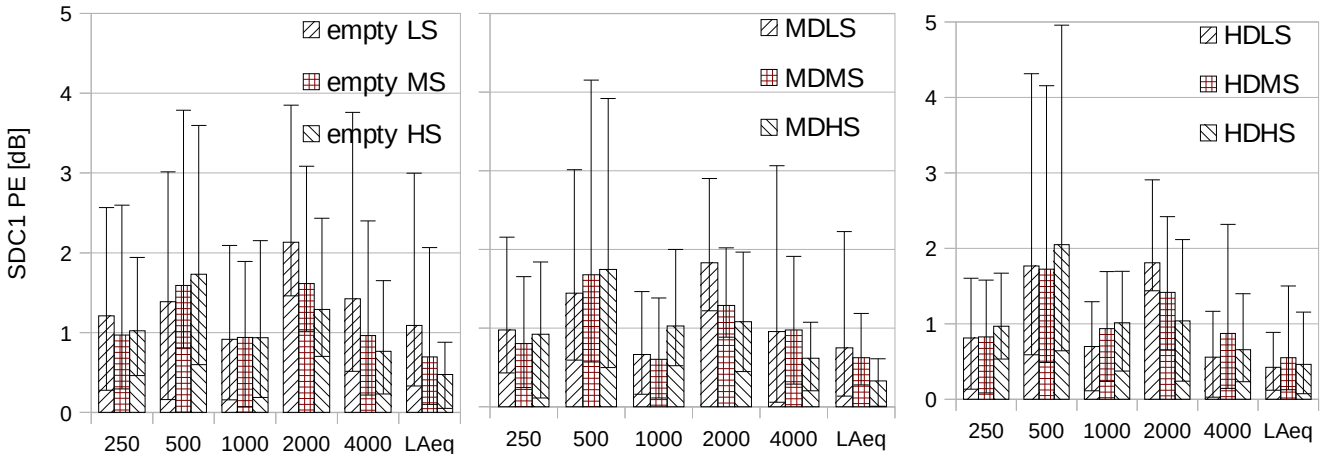

Figure 5 a-c: SDC 1 Prediction Error [dB] including 10% and 90% quantiles. Empty room, MD, HD scenario

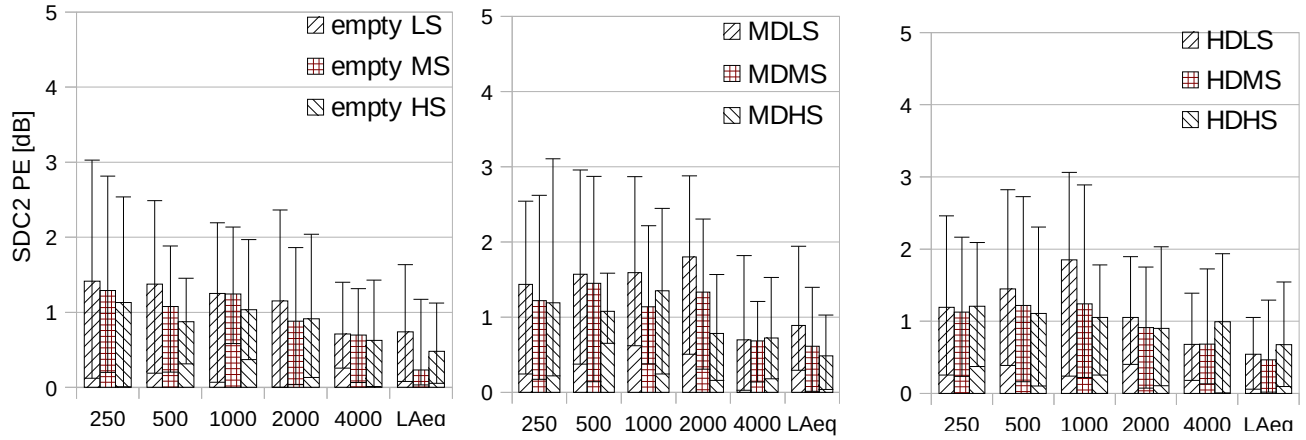

Figure 6 a-c: SDC 2 Prediction Error [dB] including 10% and 90% quantiles. Empty room, MD, HD scenario

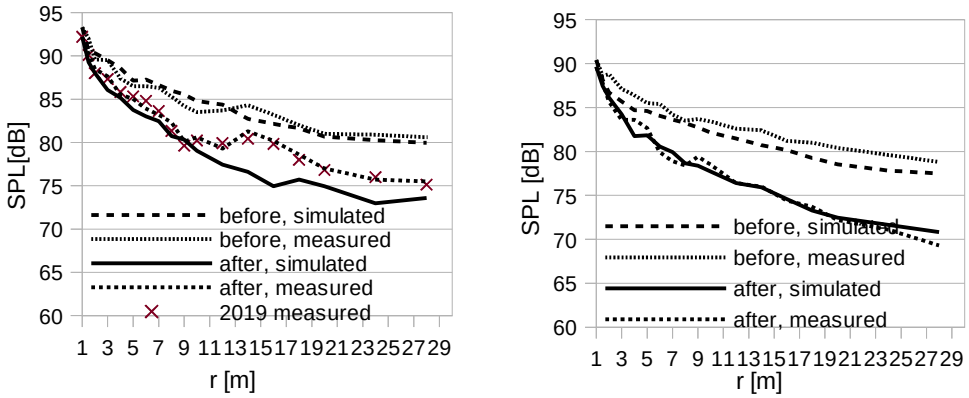

Figure 7 a,b SPL decay examples: a HDMS, SDC1, 500Hz; b: MDMS, SDC1, 1000Hz

SDC1 CE near	250	500	1000	2000	4000	LAeq
empty LS	0,2	0,2	0,7	0,5	0,4	0,4
empty MS	0,2	0,3	0,5	0,3	0,1	0,1
empty HS	0,3	0,0	0,3	0,2	0,3	0,3
MDLS	0,0	0,2	0,2	0,2	0,2	0,2
MDMS	0,4	0,2	0,3	0,0	0,1	0,1
MDHS	0,5	0,3	0,2	0,0	0,0	0,0
HDLS	0,6	0,4	0,1	0,0	0,1	0,1
HDMS	0,6	0,3	0,1	0,0	0,2	0,2
HDHS	0,6	0,6	0,1	0,0	0,1	0,0

SDC1 CE middle	250	500	1000	2000	4000	LAeq
empty LS	0,4	0,4	0,3	0,2	0,2	0,1
empty MS	0,8	1,0	0,1	0,0	0,2	0,1
empty HS	0,7	0,8	0,7	0,3	0,1	0,2
MDLS	0,3	0,8	0,3	0,2	0,3	0,1
MDMS	0,6	0,8	0,3	0,6	0,5	0,5
MDHS	1,1	1,1	0,5	0,7	0,7	0,7
HDLS	1,2	1,1	0,7	0,7	0,7	0,8
HDMS	1,3	1,0	0,8	0,6	0,4	0,6
HDHS	1,6	1,5	0,7	1,4	0,8	1,0

SDC1 PE near	250	500	1000	2000	4000	LAeq
empty LS	0,3	0,8	0,5	0,7	0,0	0,0
empty MS	0,0	0,7	0,5	0,6	0,2	0,1
empty HS	0,0	0,6	0,8	0,6	0,1	0,1
MDLS	0,0	0,6	0,4	0,7	0,0	0,0
MDMS	0,1	0,5	0,2	0,5	0,2	0,2
MDHS	0,4	0,6	0,4	0,7	0,2	0,1
HDLS	0,1	0,4	0,2	0,8	0,2	0,2
HDMS	0,5	0,4	0,5	0,9	0,2	0,2
HDHS	0,3	0,4	0,0	0,8	0,0	0,1

SDC1 PE middle	250	500	1000	2000	4000	LAeq
empty LS	0,2	0,8	0,7	0,6	2,1	1,3
empty MS	0,1	1,7	0,3	0,7	1,4	0,8
empty HS	0,5	1,4	0,8	0,3	0,7	0,1
MDLS	0,6	1,0	0,8	0,5	1,1	0,6
MDMS	0,9	1,6	0,1	0,1	1,2	0,5
MDHS	1,3	1,8	0,4	0,4	1,1	0,3
HDLS	1,0	2,4	0,3	0,1	0,8	0,1
HDMS	1,2	2,4	0,1	0,6	0,9	0,1
HDHS	1,4	2,8	1,1	0,9	0,1	0,7

SDC2 PE near	250	500	1000	2000	4000	LAeq
empty LS	0,8	0,5	0,8	0,4	0,4	0,3
empty MS	0,5	0,6	0,6	0,4	0,2	0,2
empty HS	0,4	0,6	0,5	0,6	0,0	0,1
MDLS	0,6	0,2	1,2	0,8	0,3	0,4
MDMS	0,3	0,3	0,9	0,9	0,3	0,4
MDHS	0,1	0,3	1,2	0,6	0,3	0,4
HDLS	0,3	0,0	1,2	0,6	0,3	0,4
HDMS	0,3	0,4	1,2	0,6	0,2	0,3
HDHS	0,2	0,1	0,9	0,8	0,9	0,8

SDC2 PE middle	250	500	1000	2000	4000	LAeq
empty LS	2,1	2,1	0,8	1,5	0,9	1,1
empty MS	2,0	1,7	0,5	0,4	1,0	0,9
empty HS	1,2	1,4	0,4	0,1	0,4	0,4
MDLS	1,7	2,1	0,1	1,1	0,7	0,9
MDMS	1,3	1,6	0,1	0,2	0,6	0,5
MDHS	0,9	1,0	0,5	0,1	0,3	0,1
HDLS	0,7	0,5	0,8	0,3	0,5	0,4
HDMS	0,9	1,6	0,2	0,8	0,1	0,1
HDHS	0,1	0,1	0,2	1,0	1,5	1,2

Table 3: DL2, CE and PE. Near and middle region. Values > 1 with grey background, >2 with black background.

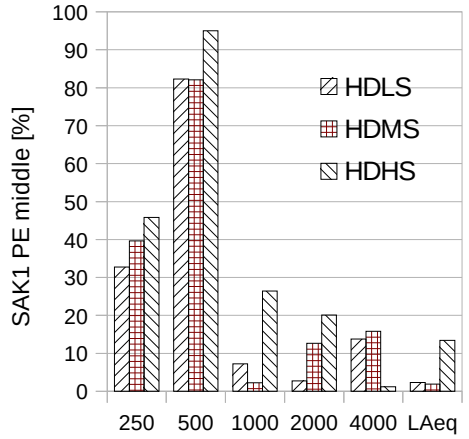

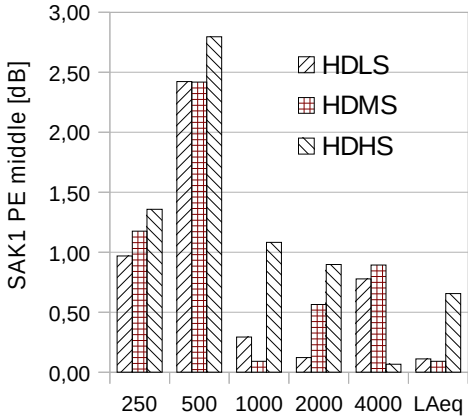

Figure 8: SDC 1 DL2 Prediction Error, Middle field, HD scenario. Figure 8a: [% measurement], Figure 8b: [dB]

	250	500	1000	2000	4000
T30 2018 – T30 2019 [%]	-5	-4	4	2	5

Table 4: Measured mean T30 Difference 2018, 2019

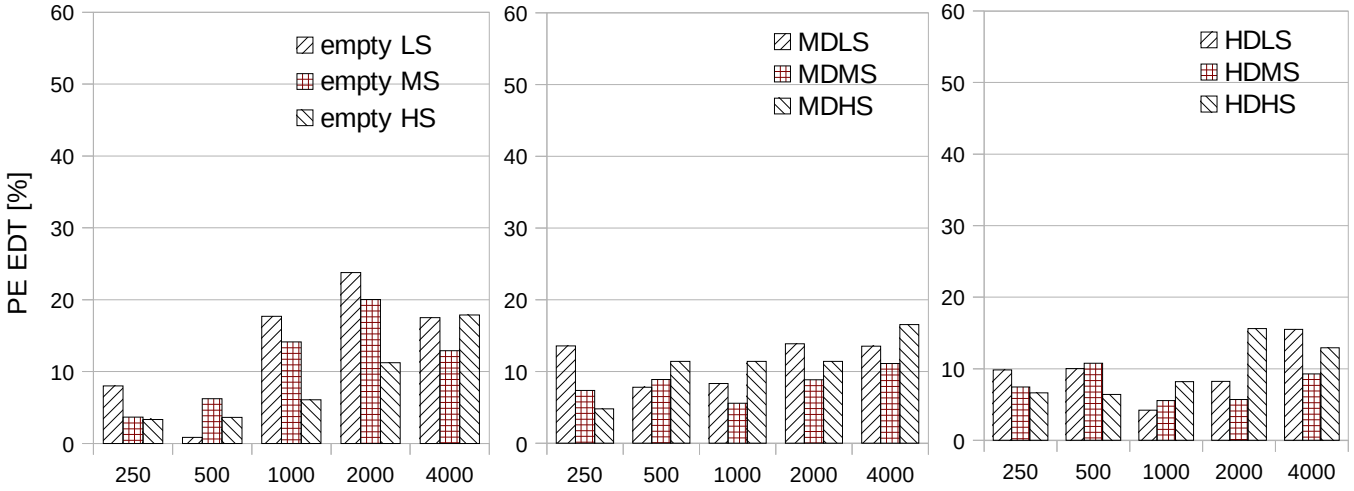

Figue 9: EDT PE [%] Measurement 2019

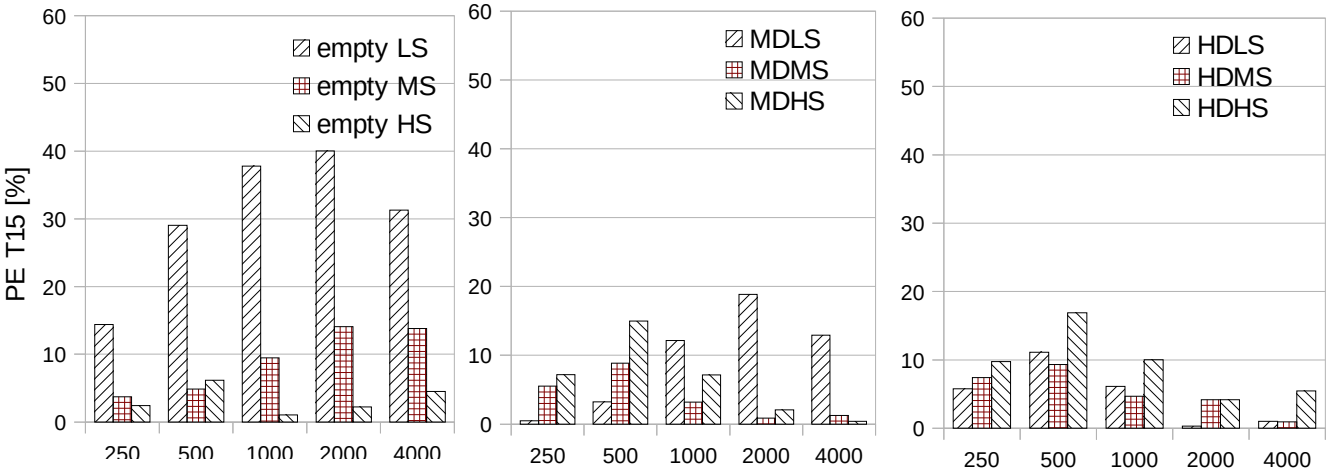

Figue 10: T15 PE [%] Measurement 2019

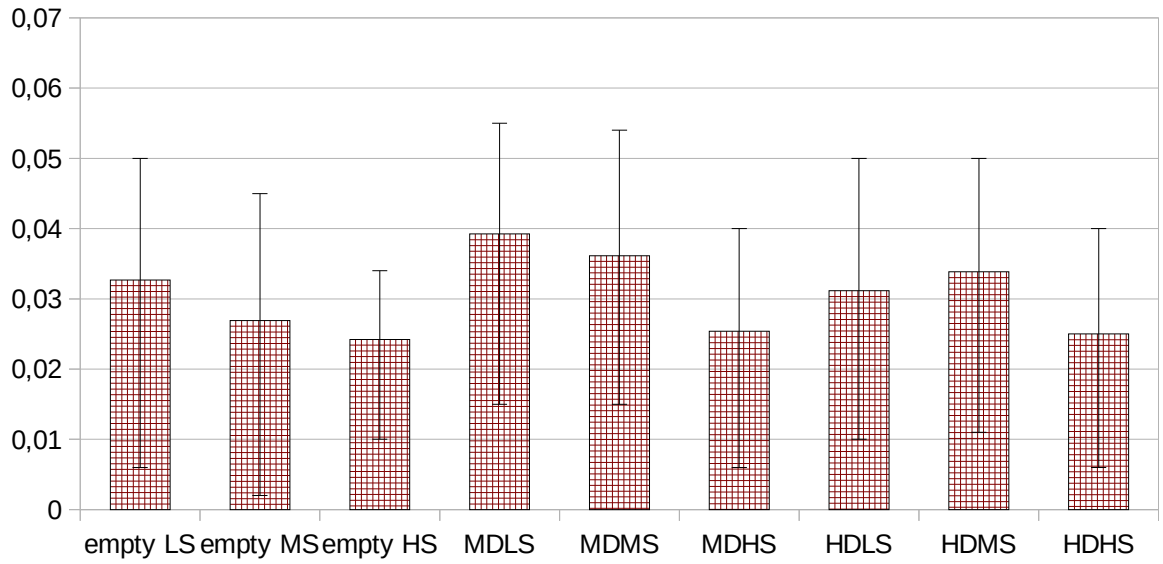

Figure 11: Mean STI PE. Error bars 10 and 90% Quantile. Measurement 2019.